Plasma Fluorination of Chemically Derived Graphene Sheets and Subsequent Modification With Butylamine

Silvia B. Bon[a)], Luca Valentini[a*)], Raquel Verdejo[b)], Jose L. Garcia Fierro[c)], Laura Peponi[a)], Miguel A. Lopez-Manchado[b)], Jose M. Kenny[a)]

a) Dipartimento di Ingegneria Civile e Ambientale, Università di Perugia, INSTM, UdR Perugia, 05100 Terni – Italy.

b) Instituto de Ciencia y Tecnologia de Polimeros, CSIC, Juan de la Cierva, 3, 28006 Madrid, Spain.

c) Instituto de Catalisis y Petroleoquimica, CSIC, Marie Curie 2, Cantoblanco, 28049 Madrid, Spain.

We describe a facile and scalable surface treatment for the functionalization of the graphene sheets (GSs). The approach consists of a surface plasma treatment of GSs by first covalently attaching fluorine and then exposing the obtained fluorinated graphene sheets (F-GSs) to a polymerization initiator such as butylamine at room temperature. Infrared and x-ray photoelectron spectroscopy have been used to demonstrate that both the fluorination of the GSs and the subsequent attachment of the amino groups to the GSs thorough the elimination of the fluorine atoms have been obtained. The successful dispersion of graphene nanosheets in organic solvents is extremely useful for their use as additives in polymer-based composites and other functional applications.

* To whom correspondence should be addressed. E-mail: mic@unipg.it.

Introduction

Graphene sheets are one-atom thick, 2D layers of sp^2-bonded carbon atoms, which can be considered as the building blocks for carbon materials such as graphite, carbon nanotubes and fullerene. Considering that graphene has been recently available for experiments[1], it is considered as a new material both for fundamental research and potential applications.

Graphene is used as a nanometer-scale building block for new nanomaterials with different device applications, such as field-effect transistors[2], resonators[3], transparent anodes[4] and organic photovoltaic devices have been reported.[5] As perfect graphene itself does not exist, the development of methods that allow processing of graphene sheets has become a top priority.

One of the strategies most used to afford single sheets of graphene relies on the graphite oxide.[6-10] Graphite oxide is heavily oxygenated, bearing hydroxyl and epoxide functional groups on their basal planes, making it strongly hydrophilic, which allows its dispersion and swelling in water. This leads to a carbon material partially oxygenated with a high specific surface area. However, the strong tendency of graphene layers to stack between each other due to van der Waals interactions prevents their solubilization in any medium. So, a critical aspect in the graphene manipulation is to maintain the sheets separated. So far, chemical functionalization of graphene has focused on improving its solubility/processability in both water and organic solvents using different soluble groups.[11-16]

We propose a novel approach to achieve stable colloidal suspensions of quasi-two-dimensional carbon sheets through plasma enhanced chemical vapour deposition. We demonstrate that the direct fluorination of graphene sheets and their subsequent derivatization provides a versatile tool for the preparation and manipulation of graphenes with variable sidewall functionalities.[16] Fluorine in graphene can be efficiently displaced by alkylamino and other functionalities leading to a nucleofilic substitution that offers an opportunity for graphenes to be integrated into the structure of different polymers, for example thermosetting polymers. Moreover the plasma functionalization of graphene represents a novel approach easy to scale up to industrial applications.

Experimental Section

Graphene sheets were produced starting from natural graphite powder (universal grade, 200 mesh, 99.9995%) as previously reported.[7] Briefly, graphite powder was dispersed in 20 mL of fuming nitric acid for 20 min; next, potassium chlorate (8 g) was slowly added over 1 h and the reaction mixture was stirred for 21 h at 0°C. The obtained graphite oxide was thermally exfoliated at 300°C for 3 min under air atmosphere giving rise to graphene sheets (GSs).

The obtained GSs were then ultrasonicated in chloroform (2mg/20mL) for 1 h. GS dispersion was drop-cast onto fluorine-doped tin-oxide (FTO)-coated glass (electrical sheet resistivity of 14 Ohm/sq). The material was then annealed at 70°C for 2 h in order to desorb any residual solvent.

Fluorinated graphene sheets (F-GSs) were obtained by the plasma assisted decomposition of CF_4 employing a 13.56 MHz radiofrequency plasma source. The plasma treatment was carried out at room temperature with the CF_4 gas pressure fixed at 10^{-2} Torr for 45 min. The CF_4 flow rate was kept constant at 21 sccm. The graphene fluorination was performed with a RF bias voltage fixed at -250 V. A commercially available grade of butylamine ($CH_3(CH_2)_3NH_2$, BAM) supplied by Sigma–Aldrich Chemicals, was used in this research. Pristine GSs and F-GSs were dispersed using an ultrasonication probe for 1 h in the liquid amine in a thermostatic bath at 5°C to avoid the evaporation of the amine.

Infrared (IR) spectroscopy (KBr pellets method), in the 500–4000 cm^{-1} range, was used to confirm the presence of covalently bound fluorine and the amino functionalization of the F-GSs.

X-ray photoelectron spectroscopy (XPS) spectra were recorded using an Escalab 200R spectrometer with a hemispherical analyzer operated on a constant pass energy mode and non-monochromatized Mg K_α X-ray radiation (hv = 1253.6 eV) at 10 mA and 12 kV. Data analysis was performed with the "XPS peak" program. The spectra were decomposed by the least squares fitting routine using a Gauss/Lorentz product information after subtracting a Shirley background.

Thermogravimetric analysis (TGA) was performed on 40 mg samples on a Seiko Exstar 6000 TGA quartz rod microbalance. The tests were done in nitrogen (250 mL*min^{-1}) from 25 °C to 900 °C with a 10 °C/min heating ramp.

The morphologies of GSs, F-GSs and amino modified F-GSs were investigated by field-emission scanning electron microscopy and atomic force microscopy (AFM) Nanocsope IV from Digital Instruments. AFM images were obtained in tapping mode. Raman spectra of samples were measured using a Renishaw Invia microscope using an excitation wavelength of 514.5 nm.

Results and Discussion

The XPS is a technique particularly suited to monitor the evolution of functional groups onto the surface of carbon-based materials.[17,18] Thus, the XPS technique was used in this work to determine the nature and the relative amount of functional groups present on the graphene surface. The C1s, O1s and F1s spectra of the samples are shown in Figure 1 and the relative amount is reported in Table 1. All peaks were decomposed into several symmetrical components (i. e. five for C1s; two for O1s and F1s).

The C1s peak was satisfactorily fitted to five components (Figure. 1a) according to the peak assignment used by Stankovich et al.[19]. The most intense peak at 284.8 eV is due to sp^2 C–C bonds of graphitic carbon. The component at 286.2 and 286.9 eV has been often assigned to C-N and C-O bonds, respectively,[19] whereas that at 288.1 and 289.4 eV to carbonyl (C=O) and carboxylic (COO) species, respectively.[16,20,21] A weak component at around 291.0 eV was also observed corresponding to $\pi \rightarrow \pi^*$ transition of carbon atoms in graphene structures.[17,22]

Samples displayed the O1s core-level spectra very broad, which means than more than one O-containing species are present (Figure 1b). A first component at 531.1–531.5 eV corresponded to O=C surface groups, and a second one placed at 532.9-533.6 eV is associated with O–C bonds[22], demonstrating the existence of functional groups on the graphene surface.

In the case of graphene treated with CF_4 plasma (Figure 1c), a peak at 290.1 eV characteristic of C-F bonds has been found.[23] More information on the nature of fluorinated C-F species can be obtained by looking at the F1s core-level. As illustrated in Figure 1d, the F1s spectrum of the CF_4-plasma treated sample was fitted to two components at 686.4 and 687.8 eV associated to C-F and CF_3 moieties,

4

respectively.[24] In addition, the N 1s peak was recorded for the plasma treated sample exposed to butylamine. Peak fitting procedure revealed two N 1s components at binding energies of 399.7 and 401.2 eV. The former major one is typical of C-N bond of butylamine whereas the later minor one comes likely from the C-N bond in protonated Bu-NH$_3^+$ moieties resulting from the interaction of amine groups with the carboxylic groups.

XPS results are corroborated by IR spectra reported in Figure 2. The spectrum of neat GS (Figure 2a) and F-GS (Figure 2b) illustrates the peaks at 1060 and 1730 cm^{-1} which are characteristics of the C-O and C=O stretches of the graphene sheets.[25] C-F vibration modes are located in the 1000–1400 cm^{-1} region, including -CF$_2$ stretching mode at 1120 cm^{-1}[26] and F-aryl mode at 1150 and 1260 cm^{-1}.[27] After the plasma treatment a band at 1260 cm^{-1} attributed to covalent C–F bonding appear (inset of Figure 2b).

Fluorine groups covalently attached to the graphenes offer the opportunity for chemical interactions with the amine systems. It was recently demonstrated that fluorine on the sidewalls of fluoronanotubes can be readily displaced by alkylidene amino groups at elevated temperature.[28] Since the chemistry of graphene is similar to that of nanotubes, these results suggested also that the F-GSs may react in situ with the amine systems.

IR spectroscopy was used to verify the occurrence of this reaction by dispersing our F-GSs in a commercial primary aliphatic amines such as butylamine at room temperature (Figure 3a). The absorptions of the primary amine at 3290 and 3370 cm^{-1}, due to asymmetric and symmetric stretching vibrations, respectively,[29] changed in the butylamine after the reaction with F-GS and formed a broad band at 3400 cm^{-1} attribute to a secondary amine. It should be mentioned that after the BAM treatment the peaks at 1060 and 1730 cm^{-1} corresponding to the C-O and C=O stretches of the graphene sheets are still visible in the IR spectra of BAM modified F-GSs while the band at 1260 cm^{-1} attributed to covalent C–F bond disappears. These findings suggest that the mechanism of interaction between fluorinated graphenes and primary amine proceeds via elimination of fluorine (Figure 3a and Table 1) and the formation of N–H bond (Figure 3b and table 1) as confirmed by C1s and N1s XPS spectra, respectively.

The C-N bonds could not be resolved because the C-N component is overshadowed by the stronger C-O component located at almost the same binding energy.[20] It should be noticed that the addition of pristine GSs to butylamine does not produce any change in the amine IR spectrum.

Field emission scanning electron microscopy was used to obtain direct visualization of our GSs and F-GSs dispersed in butylamine. The samples for the FE-SEM analysis have been prepared by drop-casting the GSs and F-GSs from chloroform solution and F-GSs dispersed in butylamine onto the FTO substrate, respectively. Representative FE-SEM images of the dried powders are shown in Figure 4. What is observed is an agglomerated powder with a "fluffy" appearance for the GSs and F-GSs (Figures 4a and 4b, respectively). After dispersing the F-GSs in butylamine using sonication, this fluffy appearance was replaced by a wrinkled thin paper-like structure (Figure 4c).

Atomic force microscopy, AFM, is one of the most direct methods of quantifying the degree of exfoliation to graphene sheet level. Tapping mode AFM image of the BAM modified F-GSs is reported in Figure 5. Amino functionalized F-GSs was previously diluted in DMF and then cast on a glass support before its observation by AFM. Well-dispersed graphene sheets have been obtained. Graphene sheets with average thickness of 0.7-0.9 nm were observed, which is characteristic of exfoliated graphene sheet.[11,12]

The thermal degradation analysis of GSs, GSs with butylamine and BAM modified F-GSs have provided further evidence for covalent functionalization. The thermogram recorded under nitrogen flow of GSs (Figure 6) shows one step of degradation at about 280 °C, which corresponds, as previously reported, to the decomposition of oxygen containing groups. This peak has been recorded also for the GSs when dispersed into the butylamine. Interesting, the derivative profile for the BAM modified F-GSs reports the loss of the degradation peak at 280°C with the appearance of a maximum of degradation at 700°C. As suggested by previous work in carbon nanotubes[30], the presence of this degradation peak at 700°C could be ascribed to a defect migration and vacancy coalescence induced by heat treatment

effects that could be taking place at this stage, forming large area defects which turn the sample into a more reactive material as confirmed by the IR analysis performed on F-GSs dispersed in butylamine.

This hypothesis was confirmed by Raman spectroscopy (Figure 7) where the presence of two broad bands extending between 1355 cm^{-1} and 1575 cm^{-1}, usually referred as to D (breathing modes of sp^2 atoms in rings[31-33]) and G (graphitic, sp^2 bonded carbon) peaks, and their relative intensity ratio (I_D/I_G) gives an indication of the degree of disorder in carbon based materials.[34-36] In general it was observed that a larger degree of disorder was observed on BAM modified F-GSs (legend of Figure 7).

Conclusions

We have developed a novel approach easy to scale up to industrial application for fluorine functionalization of graphene sheets with CF$_4$ plasma treatment. Fluorine atoms have been attached to graphene through the C–F covalent bond leading to a stable dispersion of individual graphene sheets when they were exposed to organic moieties. The applications of F-GSs prepared in the present work suggest the possibility of using amino-functionalized GSs in a broad range of polycondensation reactions leading to the production of new covalently integrated graphene-reinforced thermosetting polymers. These studies are currently in progress in our laboratory.

References

(1) Geim, A. K.; Novoselov, K. S. *Nature Mater.* **2007**, *6*, 183.

(2) Novoselov, K. S.; Geim, A. K.; Morozov, S. V.; Jiang, D.; Zhang, Y.; Dubonos, S. V.; Grigorieva, I. V.; Firsov, A. A. *Science* **2004**, *306*, 666.

(3) Bunch, J. S.; van der Zande, A. M.; Verbridge, S. S.; Frank, I. W.; Tanenbaum, D. M.; Parpia, J. M.; Craighead, H. G.; Mceuen, P. L. *Science* **2007**, *315*, 490.

(4) Becerril, H. A., Mao, J.; Liu, Z. F.; Stoltenberg, R. M.; Bao, Z. N.; Chen, Y. S. *ACS Nano* **2008**, *2*, 463.

(5) Liu, Z. F.; Liu, Q.; Zhang, X. Y.; Huang, Y.; Ma, Y. F.; Yin, S. G.; Chen, Y. S. *Adv. Mater.* **2008**, *20*, 3924.

(6) Stankovich, S.; Dikin, D. A.; Dommett, G. H. B.; Kohlhaas, K. M.; Zimney, E. J.; Stach, E. A.; Piner, R. D.; Nguyen, S. T.; Ruoff, R. S. *Nature* **2006**, *442*, 282.

(7) Verdejo, R.; Barroso-Bujans, F.; Rodriguez-Perez, M. A.; de Saja, J. A.; Lopez-Manchado, M. A. *J. Mater. Chem.* **2008**, *18*, 2221.

(8) Schniepp, H. C.; Li, J. L.; McAllister, M. J.; Sai, H.; Herrera-Alonso, M.; Adamson, D. H.; Prudhomme, R. K.; Car, R.; Saville, D. A.; Aksay, I. A. *J. Phys. Chem. B* **2006**, *110*, 8535.

(9) Gilje, S.; Han, S.; Wang, M.; Wang, K. L.; Kaner, R. B. *Nano Lett.* **2007**, *7*, 3394.

(10) Gomez-Navarro, C.; Weitz, R. T.; Bittner, A. M.; Scolari, M.; Mews, A.; Burghard, M.; Kern, K. *Nano Lett.* **2007**, *7*, 3499.

(11) Niyogi, S.; Bekyarova, E.; Itkis, M. E.; McWilliams, J. L.; Hamon, M. A.; Haddon, R. C. *J. Am. Chem. Soc.* **2006**, *128*, 7720.

(12) Xu, Y. X.; Bai, H.; Lu, G. W.; Li, C.; Shi, G. Q. *J. Am. Chem. Soc.* **2008**, *130*, 5856.

(13) Stankovich, S.; Dikin, D. A.; Dommett, G. H. B.; Kohlhaas, K. M.; Zimney, E. J.; Stach, E. A.; Piner, R. D.; Nguyen, S. T.; Ruoff, R. S. *Nature* **2006**, *442*, 282.

(14) Stankovich, S.; Piner, R. D.; Nguyen, S. T.; Ruoff, R. S. *Carbon* **2006**, *44*, 3342.

(15) Si, Y. C.; Samulski, E. T. *Nano Lett.* **2008**, *8*, 1679.

(16) Eda, G.; Fanchini, G.; Chhowalla, M. *Nat. Nanotechnol.* **2008**, *3*, 270.

(17) Boehm, H. P. *Carbon* **2002**, *40*, 145.

(18) Lennon, D.; Lundie, D. T.; Jackson, S. D.; Kelly, J. P.; Parker, S. F. *Langmuir* 2002, *18*, 4667.

(19) Stankovich, S.; Dikin, D. A.; Piner, R. D.; Kohlhaas, K. A.; Kleinhammes, A.; Jia, Y.; Wu, Y.; Nguyen, S. T.; Ruoff, R. S. Carbon 2007, 45, 1558.

(20) Stankovich, S.; Dikin, D. A.; Piner, R. D.; Kohlhaas, K. A.; Kleinhammes, A.; Jia, Y.; Wu, Y.; Nguyen, S. T.; Ruoff, R. S. *Carbon* **2007**, *45*, 1558.

(21) Bekyarova, E.; Itkis, M. E.; Ramesh, P.; Berger, C.; Sprinkle, M.; de Heer, W. A.; Haddon, R. C. *J. Am. Chem. Soc.* **2009**, *131*, 1336.

(22) Okpalugo, T. I. T.; Papakonstantinou, P.; Murphy, H.; McLaughlin, J.; Brown, N. M. D. *Carbon* **2005**, *43*, 153.

(23) Ramdutt, D.; Charles, C.; Hudspeth, J.; Ladewig, B.; Gengenbach, T.; Boswell, R.; Dicks, A.; Brault, P. *J. Power Sources* **2007**, *165*, 41.

(24) Briggs, D.; Seah, M. P. In *Practical Surface Analysis. Auger and X-ray Photoelectron Spectroscopy*; 2nd Ed.; John Wiley and Sons: Chischester, 1990.

(25) Liang, Y.; Wu, D.; Feng, X.; Mullen, K. *Adv. Mater.* **2009**, *21*, 1.

(26) Khare, B. N.; Wilhite, P.; Meyyappan, M. *Nanotechnology* **2004**, *15*, 1650.

(27) Felten, A.; Bittencourt, C.; Pireaux, J. J. *J. Appl. Phys.* **2005,** *98*, 093123.

(28) Stevens, J. L.; Huang, A. Y.; Peng, H.; Chiang, I. W.; Khabashesku, V. N.; Margrave J. L. *Nano Lett.* **2003**, *3*, 331.

(29) Williams, D. H.; Fleming, I. In *Spectroscopic Methods in Organic Chemistry*, McGraw-Hill Companies, 1969.

(30) Jin, C.; Suenaga, K.; Iijima, S.; *Nano Lett.* **2008**, *8*, 1127.

(31) Tuinstra, F.; Koenig, J. L.. *J. Chem. Phys.* **1970**, *53*, 1126.

(32) Ferrari, A. C.; Robertson,J.. *Phys. Rev. B* **2000**, *61*, 14095.

(33) Worsley, K. A.; Ramesh, P.; Mandal, S. K.; Niyogi, S.; Itkis, M. E.; Haddon, R. C. *Chem. Phys. Lett.* **2007**, *445*, 51.

(34) Plank, N. O. V.; Jiang, L. D.; Cheung, R. *Appl. Phys. Lett.* **2003**, *83*, 2426.

(35) Valentini, L.; Puglia, D.; Carniato, F.; Boccaleri, E.; Marchese, L.; Kenny, J. M. *Composites Science and Technol.* **2008**, *68*, 1008.

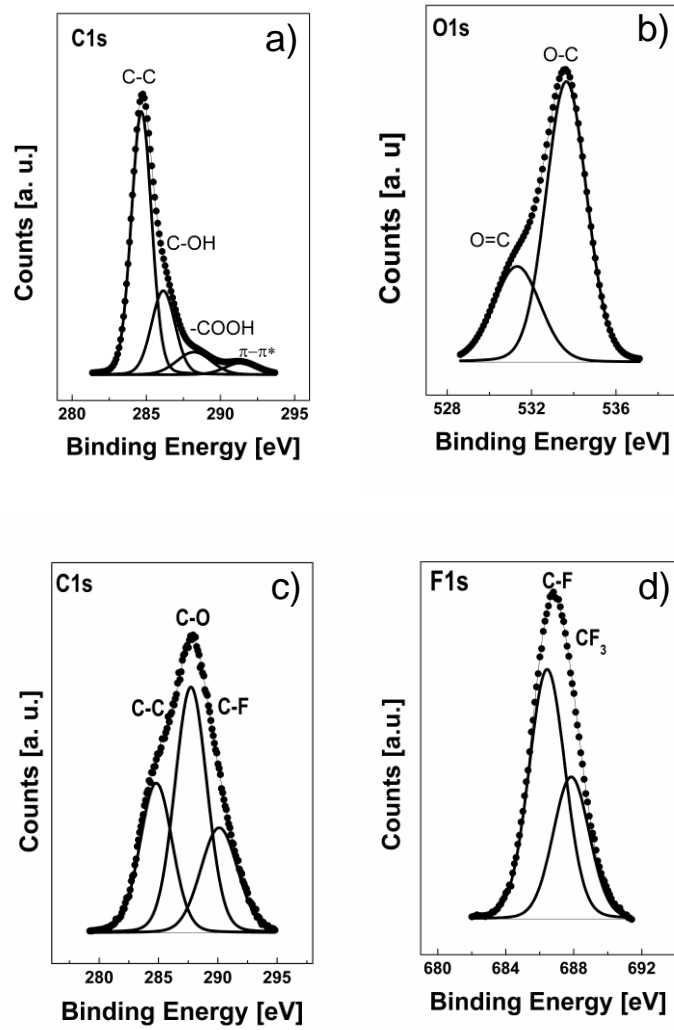(36) Kudin, K.; Ozbas, B.; Schniepp, H.; Prud'homme, R.; Aksay, I.; Car, R. *Nano Lett.* **2008**, *8*, 36.

Figure 1: (a) C1s and (b) O1s XPS spectra of GSs. (c) C1s and (d) F1s XPS spectra of F-GSs.
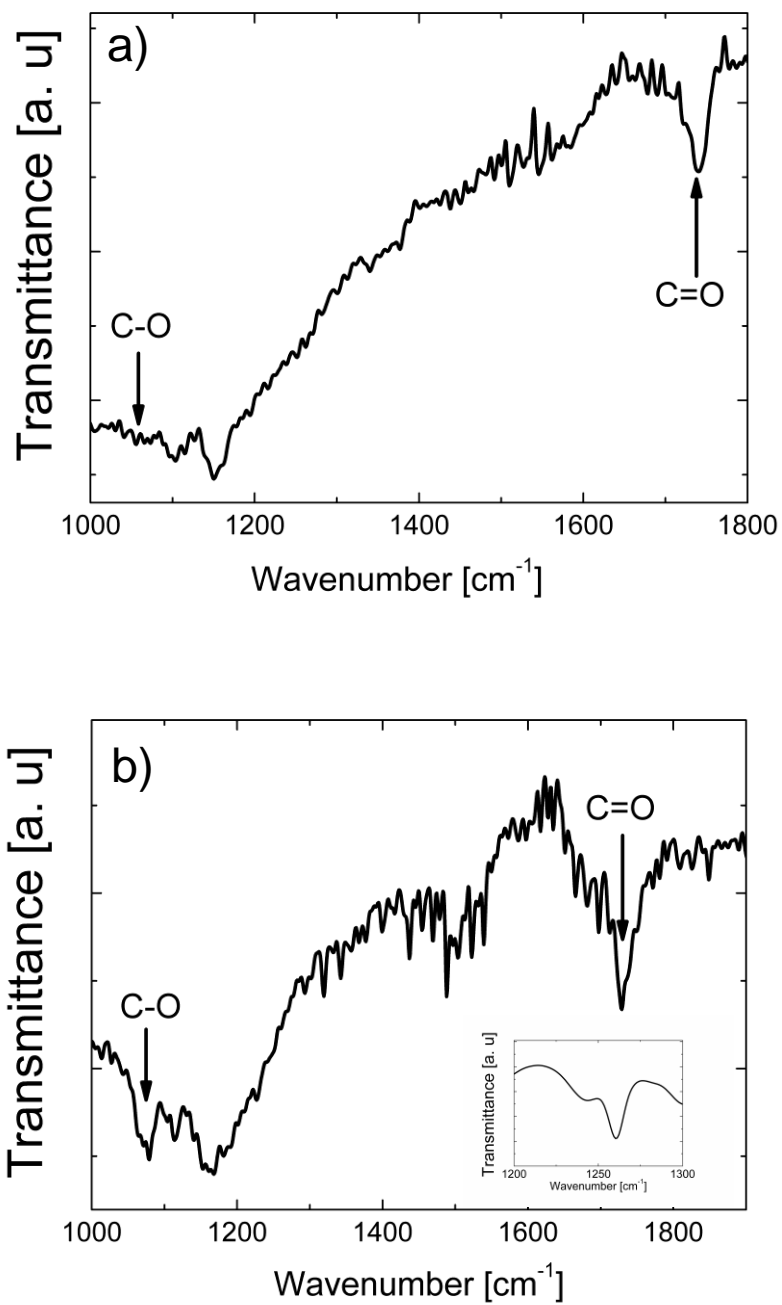
Figure 2: IR spectra of (a) GSs and (b) F-GSs. The inset shows an enlargement of the IR spectrum of the F-GSs.
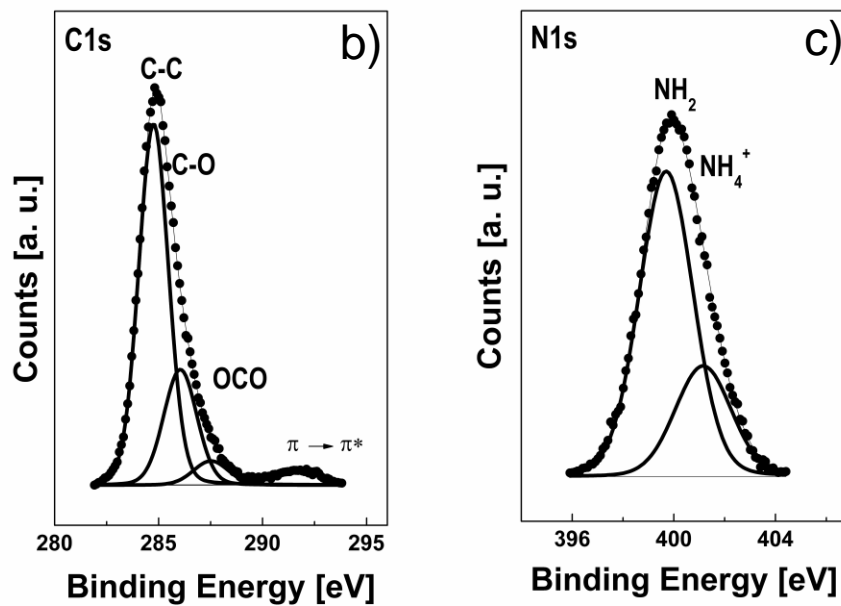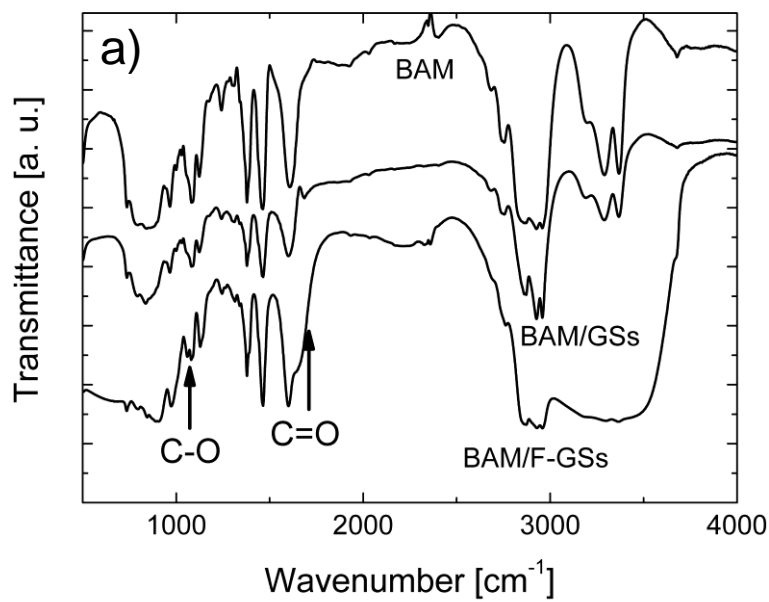
Figure 3: (a) IR spectra of BAM, GS derivatives produced by the addition of butylamine (BAM/GSs) and F-GS derivatives produced by reactions with butylamine (BAM/F-GSs). (b) C1s and (c) N1s XPS spectra of BAM modified F-GSs.
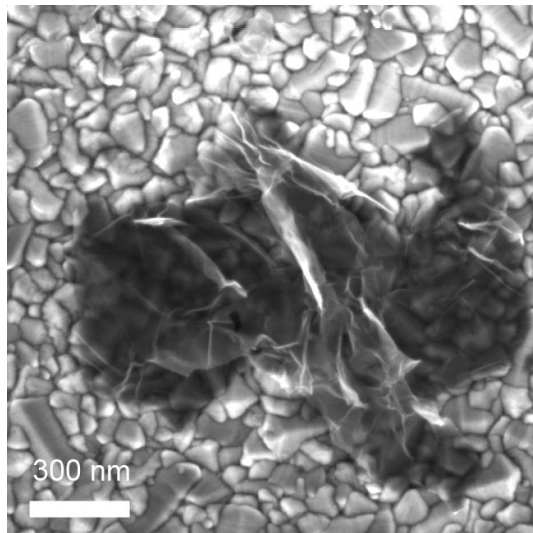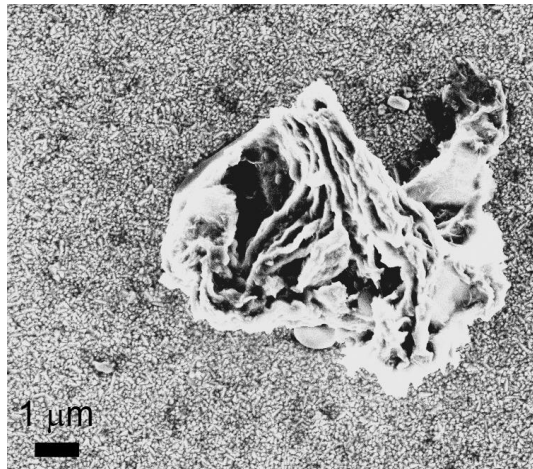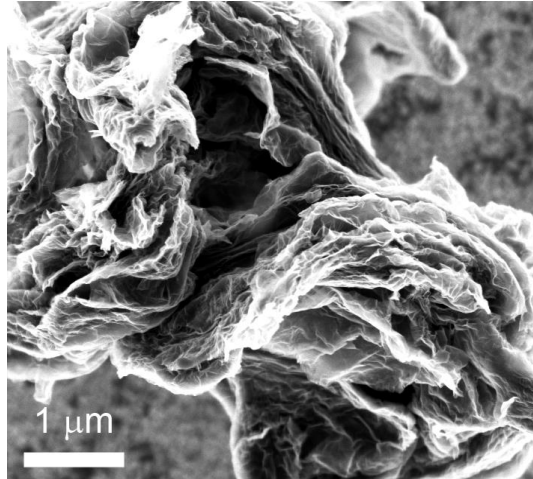
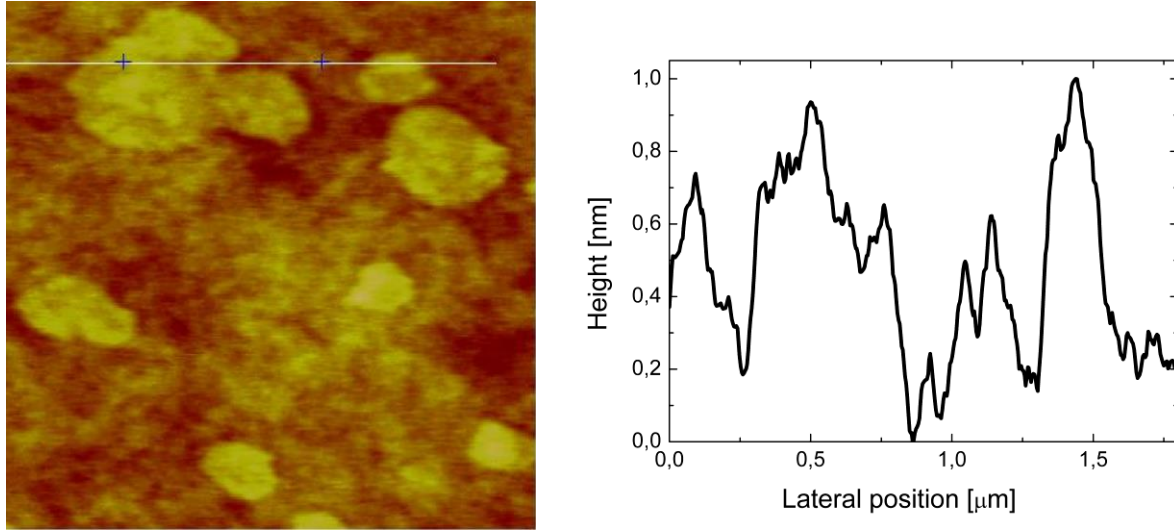Figure 4: FE-SEM images for (a) neat GSs, (b) F-GSs and (c) BAM modified F-GSs.

Figure 5: 2D tapping-mode topography (2 μm X 2 μm) AFM image and normalized height profile of the BAM modified F-GSs.
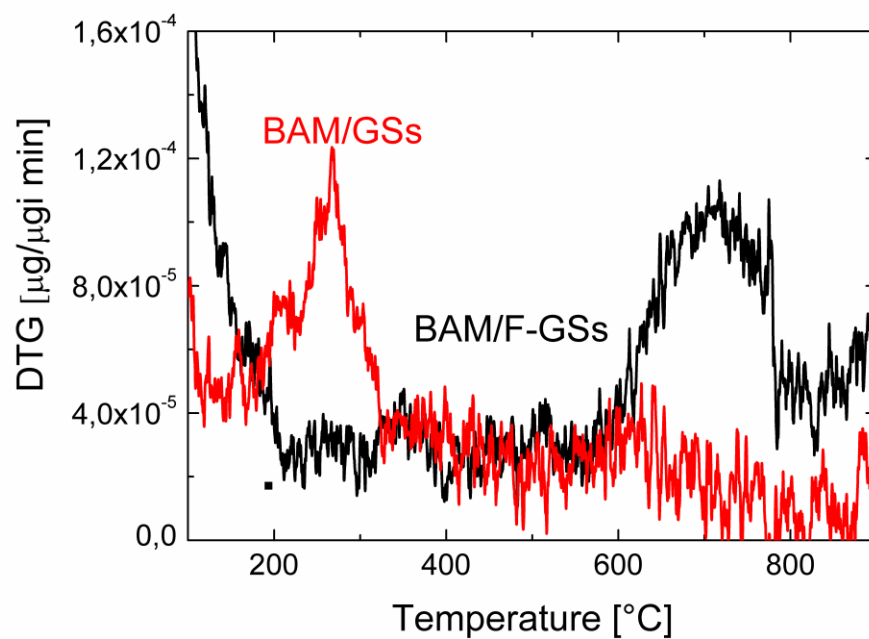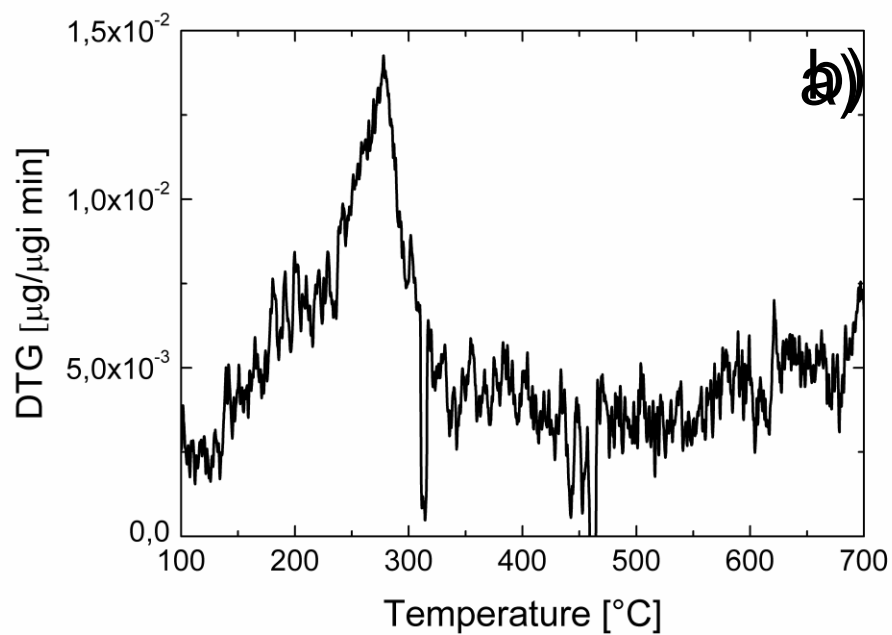
Figure 6: Derivative thermograms of pristine (a) GSs and (b) GSs dispersed in BAM (BAM/GSs) and BAM-functionalized F-GS (BAM/F-GSs) in nitrogen atmosphere.
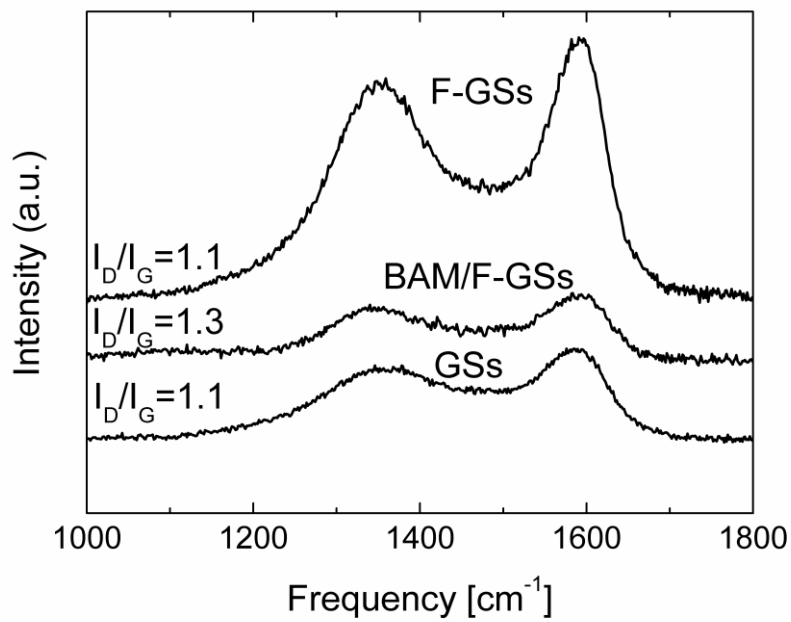
Figure 7: Raman spectra of GSs, F-GSs and BAM modified F-GSs (BAM/F-GSs).

Table 1: Peak assignment (between parentheses), Binding energy peaks and atomic percentage (between parentheses in bold) for the analyzed samples.

Samples	C1s	N1s	O1s	F1s	At/C
GSs	C-C 284.8 (**65**) C-OH 286.5 (**23**) -COOH 288.6 (**12**)	-	C=O 531.3 (**28**) C-O 533.6 (**72**)	-	O/C 0.101
F-GSs	C-C 284.8 (**29**) C-O 287.7 (**47**) C-F 290.1 (**24**)	-	C=O 531.6 (**32**) C-O 532.9 (**68**)	C-F 686.4 (**64**) CF_3 687.8 (**36**)	F/C 0.899
BAM modified F-GSs	C-C 284.8 (**67**) C-N 286.2 (23) C-O 286.8 (**4**) C=O 288.1 (4) OCO 289.6 (**2**)	NH_2 399.7 (**73**) NH_4^+ 401.2 (**27**)	C=O 531.6 (**51**) C-O 532.9 (**49**)	-	N/C 0.065